Available online at www.scholarsresearchlibrary.com

Scholars Research Library

Archives of Applied Science Research, 2012, 4 (5):2040-2051
(http://scholarsresearchlibrary.com/archive.html)

ISSN 0975-508X
CODEN (USA) AASRC9

Essence of Mechanical Properties from Variable Growth Habits of Binary, Ternary and Quanternary Aluminium Rich Alloys

Parshotam Lal, Shallu Abrol and B. L. Sharma

ISCAS Institute of Solid State and Materials Science, Jammu University Campus, Jammu-180 006, India

---

ABSTRACT

Composite alloys Al-Cd; Al-Cd-Bi and Al-Cd-Bi-Pb are characterized by thermal, X-ray and microscopic studies. The composite alloys are grown at different modes of solidification to understand comprehensively the intrarelationship among Lamellae of the constituent materials comprising their respective solidus structures. X-ray diffraction studies affirm composite alloys to be a terminal solidus solution of physically distinct and mechanically separable phases. Growth habits and thermal stability of composite phases are ascertained using SEM and DSC. The variation of an anisotropic mechanical property over the entire experimental range of growth velocity furnishes an evidence of its dependence as linear, non-linear and linear respectively, in the slow, moderate and fast growth regions of solidification. Evidentially, this generates the strength-growth relationship which follows an identical form of the Weibull probability distribution curve inculcating the obedience of microstructural parameters to the distribution. Consequently, the curve has two cut-off points corresponding to a lower strength limit in the slow and fast growth regions and an upper strength limit in the moderate growth region. The latter is equivalent to the theoretical strength of lamellae, as microstructural parameters obey Gauss distribution in the absence of any surface flaws which are responsible for the reduced strength. Moderate anisotropic growth velocity (~2.90 x 10^{-7} m^3s^{-1}) strengthens the composite microstructures two to three fold of their isotropic growth observed in an icebath (~273 K) and manifold superior to their constituent phases irrespective of growth mode.

Keywords: Mechanical parameters, crystal lamellae, fracture toughness, growth habits.

INTRODUCTION

The essence of moderate anisotropic growth applied to composite materials is the ability to put strong stiff fibers in the right place, in the right orientation with right volume fraction. Implicit in the present searching approach is the concept by the solidification process discover the final product as an acceptable analog for manufacturing the engineering product [1-5]. Because of the complex nature of the phenomena involved in an anisotropic growth process from the melt, a considerable judgment is required to assess both theoretical and experimental observations, since the composite materials that can be developed by this process exhibit a large diversity of micro-morphologies[6-9]. However, a physical understanding of the mechanical properties of composite materials as a basis for the improvement of the properties by controlling the growth rate from the melt can readily be distinguished when examined in an optical or electronic microscope. The current work is conducted on aluminium rich composites, since aluminium in combination with Ti and V is commonly used for the femoral stem component of the prosthetic hip joints. Aluminium and its alloys are characterized by a relatively low density (2.7gcm^{-3} as compared to 7.9gcm^{-3} for steel), high electrical and thermal conductivities, and resistance to corrosion in some common environments, including the ambient atmosphere. Many of these alloys are easily formed by virtue of high ductility; this is evidenced by the thin aluminium foil sheet into which the relativity pure material may be rolled. The

mechanical strength of aluminium may be enhanced by cold work and by alloying; however, both processes tend to diminish resistance to corrosion.

Recent attention has been focused on aluminium alloys and other low density metal (e.g Mg, Ti) as engineering meterials for transportation, to effect reductions in fuel consumption. An important characteristic of materials is specific strength, which is quantified by tensile strength- specific gravity ratio. Though an alloy of one of these metals may have a tensil strength that is inferior to a more dense material (such as steel), on a weight basis, yet it will be able to sustain a large load. A generation of new aluminium-lithium alloys have been developed recently for use by the aircraft aerospace industries. These materials have relatively low densities (between about 2.5 and 2.6gcm^{-3}) high specific moduli (elastic modulus-specific gravity ratios), and excellent fatigue and low-temperature toughness properties [5]. The main aesthetics and motivation of the present investigation is to reveal the concept that the moderate anisotropic growth of the composite phases from their respective liquidus phases could produce modal products [7-12] with unique properties as acceptable analogs for manufacturing engineering products.

MATERIALS AND METHODS

i) Materials and their thermal revealation

The composite alloys Al-Cd; Al-Cd-Bi and Al-Cd-Bi-Pb were prepared in the pyrex tubes by weighing variable amounts of purity 99.999% Al[Alfa Aesar, AR, mp 949 K, $\Delta_f H$ = 10.80 kJmol^{-1}], 99.999% Cd [Alfa Aesar, AR, mp 597.0 K, $\Delta_f H$ = 6.19 kJmol^{-1}], 99.999% Bi (Alfa Aesar, AR, mp 551 K, $\Delta_f H$ = 11.20 kJmol^{-1}and 99.999% Pb[Alfa Aesar, AR, mp 584 K, $\Delta_f H$ = 4.70 kJmol^{-1}) shots with 60 wt% Al and 40 wt% Cd; 40 wt% Al, 30 wt% Cd and 30 wt% Bi and 40 wt% Al, 20wt% Cd, 20 wt% Bi and 20 wt% Pb respectively. The melting temperatures and enthalpies of fusion of the constituent matels, cited in the parentheses, were obtained by thermal analysis approaching very closely to their literature values. The ampoule tubes were sealed under vacuum to avoid oxidation and subsequently infused in a furnace set at a temperature ~ 1000 K for alloying Al, Cd, Bi and Pb metals. Homogeneity of the alloys were ensured by heat-chill process keeping the temperature of the heater (air oven) ~ 700 K and that of the cooler (water bath) ~300 K. The liquidus temperatures of the composite alloys Al-Cd (596.90 K), Al-Cd-Bi (429.20 K) and Al-Cd-Bi-Pb (370.50 K) were also ascertained by thermal analysis.

ii) Oriented growth

Anistropic solidification composite of the composite alloys and their constituent metals from respective molten state was achieved in the following experimental setup. An experimental sealed pyrex tube containing half-full melt of a freshly prepared composite or metal, was clamped to the centre of an empty graduated beaker (volume capacity ~1dm^3) manipulated midmost in an air oven set at a temperature 30K higher than the melting temperature of the samples. The molten mass in the tube was nucleated by circulating silicone oil at 18 different intervals spanned in the time range 50-60 min. from the oil reservoir perforated and plugged with a glass tube carrying valve to control the percolation at ~300K. The melt in the tube started nucleating when the rising level of the oil just touched the bottom of the tube. Several samples of the composites and constituent metals were grown anistropically at different but nearly consistent growth rates determined by circulating approximately the same volume of the oil for the aforementioned intervals.

Isotropic growth was performed by immersing an experimental pyrex tube containing the composite or metal melt in an ice bath maintained at ~ 273 K. The growth being instantaneous in nature, is presumed of zero order. Likewise, a good many samples of composite phases were solidified for the isotropic growth for observations.

iii) Rupture tests

The experimental samples after dimensions' measurement, were subsequently subjected to tensile, modulus of rupture (flexural strength) and compressive tests in a VEB Thuringer Industrie Werk Rauenstein Tensometer, whereby, a steadily increasing load would determine the rupture force of an experimental sample until it shows no ability for further resistance. Mechanical parameters of the composite phases for moderate anisotropic and isotropic modes of growth computed by the following standard relations [5,9,13-14]:

i) Modulud of rupture, $Y_{rup} = \frac{PL}{\pi r^3}$ (1)

ii) Tensile strength, $T_{rup} = \frac{P}{\pi r^2}$ (2)

iii) Compressive strength, $\sigma_{rup} = \frac{P}{\pi r^2}$ (3)

where P is the applied load in Newton force; L and r respectively are the span and radius of a specimen in m.

iv) Microscopic studies

The specimen grown anisotropically and isotropically were polished at room temperature following a procedure similar to that adopted for analogous problem [11] To reveal the microstructure, a thin layer of the specimen etched in ferric chloride was mounted on stub with gold-coated holder and examined under a scanning electron microscope for micro growth observation. Many samples of each specimen were viewed in this manner and the growth habits of the growing phases during solidification at different growth rates were accordingly photographed.

v) X-ray diffraction studies

The X-ray diffraction patterns exhibited by the experimental composite phases were recorded with Diffraction System-XPERT=PRO using Cuk$_\alpha$ radiation of wavelength1.5408 Å at room temperature.

RESULTS AND DISCUSSION

The DSC curves resulted, in by the thermal analysis of the composite alloys Al-Cd; Al-Cd-Bi and Al-Cd-Bi-Pb are presented in Fig. 1 (a,b,c) explicitly exhibiting their thermal stability, homogeneity and liquidus temperatures.

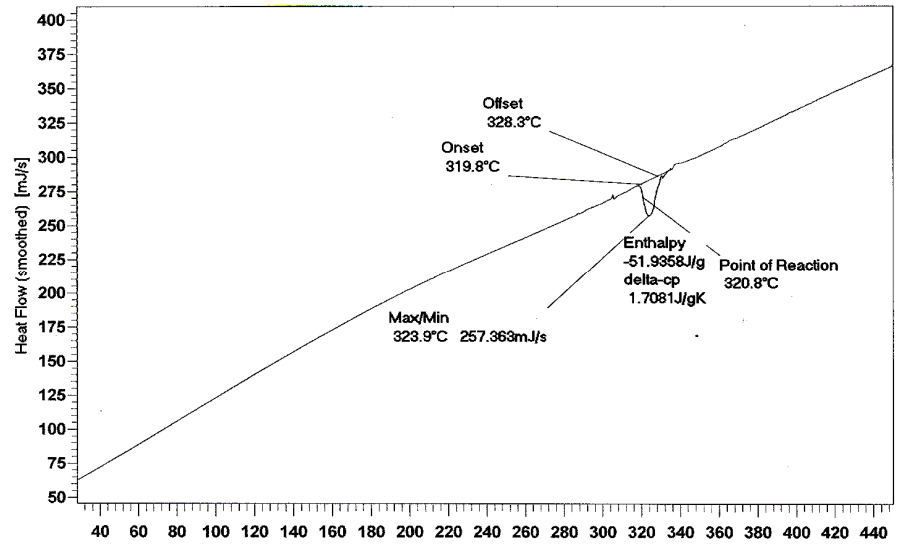

(a)

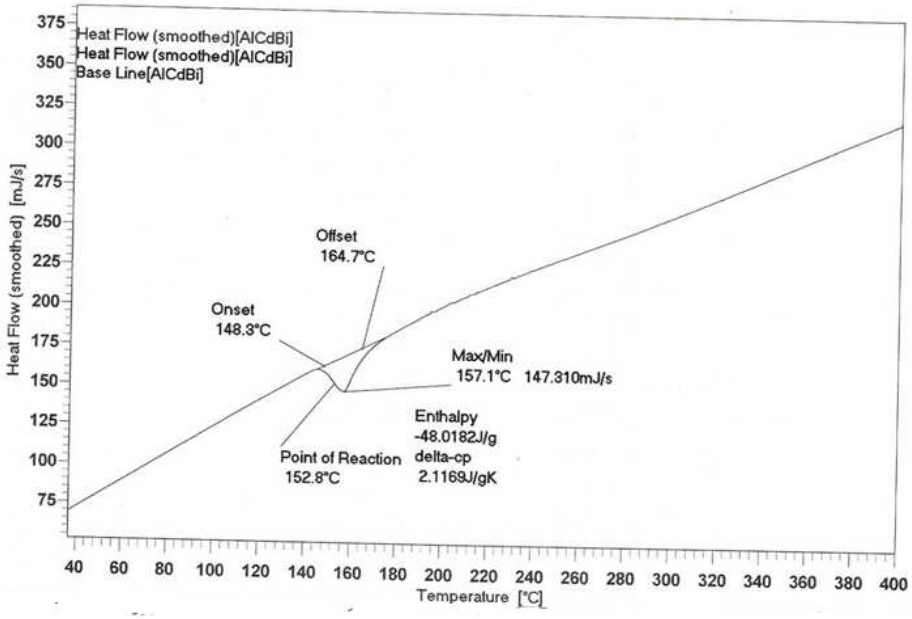

(b)

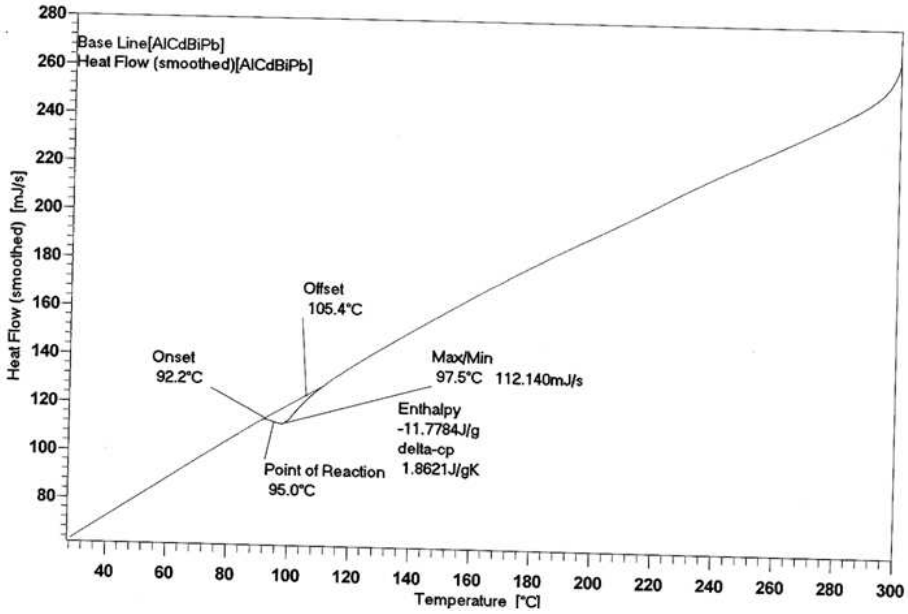

(c)

Fig.1: DSC curves of composite alloys (a) Al-Cd; (b) Al-Cd-Bi and (c) Al-Cd-Bi-Pb

The XRD data summarized in Table 1(a, b, c) and X-ray patterns represented by Fig.2(a,b,c) for composite alloys Al-Cd; Al-Cd-Bi and Al-Cd-Bi-Pb exhibit sharp lines of atomic intensities of their individual constituent phases; i.e., aluminium, cadmium, lead and bismuth. The analysis of the X-ray data and patterns implicitly, confirms the composite alloys as mechanical mixtures of their constituent phases simulating weak interactions at atomic levels. This implies that the composite alloys are terminal solidus solutions, since no unique peak or atomic intensity is observed in the analysis.

Table 1: XRD data of composite alloys (a) Al-Cd; (b) Al-Cd-Bi and (c) Al-Cd-Bi-Pb

(a)

Pos. [°2TH.]	d-spacing [Å]	Intensity[Å]	Intensity [%]	Planes (hkl)
31.835	2.808	21.4	34.5	Cd(002)
34.727	2.581	12.7	20.6	Cd(100)
38.378	2.343	61.9	10.0	Al(111)
44.711	2.025	12.9	20.8	Al(200)
47.846	1.899	96.9	15.6	Cd(102)
61.120	1.515	11.8	19.1	Cd(103)
62.284	1.489	74.3	12.0	Cd(112)
65.101	1.431	71.4	11.5	Al(220)
66.573	1.403	34.7	5.6	Cd(004)
71.661	1.315	94.4	15.2	Cd(112)
73.335	1.289	32.6	5.3	Cd(200)
75.810	1.253	43.9	7.1	Cd(201)
77.318	1.233	35.1	5.7	Cd(104)
78.252	1.220	64.0	10.3	Al(311)
82.179	1.172	34.2	5.5	Cd(200)
82.454	1.168	40.2	6.5	Al(222)

(b)

Pos. [°2TH.]	d-spacing [Å]	Intensity[Å]	Intensity [%]	Planes (hkl)
22.476	3.9525	68.0	8.2	Bi(003)
27.206	3.2751	441.0	52.7	Bi(012)
31.885	2.8044	191.0	22.9	Cd(002)
34.771	2.5780	109.0	13.0	Cd(100)
38.010	2.3654	224.0	26.8	Bi(104)
38.468	2.3383	837.0	100.0	Al(111)
39.664	2.2704	235.0	28.0	Bi(110)
44.756	2.0232	293.0	35.0	Al(200)
45.959	1.9730	84.0	10.1	Bi(008)
47.860	1.8990	81.0	9.7	Cd(102)

48.744	1.8667	122.0	14.6	Bi(202)
55.347	1.6585	25.7	3.1	Bi(024)
59.340	1.5561	33.9	4.1	Bi(103)
61.134	1.5147	104.0	12.4	Bi(200)
62.283	1.4895	119.0	14.2	Cd(112)
64.555	1.4424	127.0	15.2	Bi(122)
65.141	1.4308	136.0	16.2	Al(220)
66.538	1.4042	39.8	4.8	Cd(004)
67.502	1.3864	35.9	4.3	Bi(018)
70.829	1.3292	71.6	8.6	Bi(214)
71.678	1.3156	82.5	9.9	Cd(112)
71.904	1.3120	78.8	9.4	Bi(300)
73.763	1.2834	29.0	3.5	Bi(027)
75.600	1.2567	62.2	7.4	Bi(125)
76.461	1.2447	25.5	3.0	Cd(201)
77.323	1.2330	31.1	3.7	Cd(104)
78.266	1.2205	126.0	15.1	Al(311)
78.503	1.2174	80.3	9.6	Bi(303)
82.180	1.1720	33.6	4.0	Cd(202)
82.489	1.1684	51.8	6.2	Al(222)
85.363	1.1362	43.7	5.2	Bi(220)
85.665	1.1330	28.7	3.4	Bi(100)
87.135	1.1176	31.4	3.8	Bi(213)
89.647	1.0927	36.9	4.4	Bi(222)

(c)

Pos. [°2TH.]	d-spacing [Å]	Intensity[Å]	Intensity [%]	Planes (hkl)
22.539	3.9416	42.1	5.6	Bi(003)
27.282	3.2662	302.0	40.3	Bi(012)
31.943	2.7994	62.4	8.3	Cd(002)
34.846	2.5725	51.8	6.9	Cd(100)
38.586	2.3314	749.0	100.0	Al(111)
39.746	2.2660	167.0	22.3	Bi(110)
44.462	2.0359	85.8	11.5	Bi(016)
44.850	2.0192	324.0	43.3	Bi(008)
46.148	1.9654	41.8	5.6	Bi(113)
46.873	1.9367	30.1	4.0	Bi(021)
47.951	1.8956	41.2	5.5	Cd(102)
52.256	1.7491	76.2	10.2	Pb(220)
56.158	1.6365	70.6	9.4	Bi(024)
61.901	1.4977	93.4	12.5	Bi(200)
62.333	1.4884	74.1	9.9	Cd(112)
63.389	1.4661	63.9	8.5	Bi(211)
64.310	1.4473	67.5	9.0	Bi(122)
65.219	1.4293	156.0	20.9	Al(220)
70.907	1.3280	48.8	6.5	Bi(214)
71.724	1.3148	40.2	5.4	Bi(300)
75.674	1.2557	36.3	4.9	Bi(125)
78.343	1.2195	159.0	21.2	Al(311)
82.565	1.1675	61.7	8.2	Al(222)
87.266	1.1163	48.9	6.5	Bi(213)
89.703	1.0922	33.6	4.5	Bi(222)

(a)

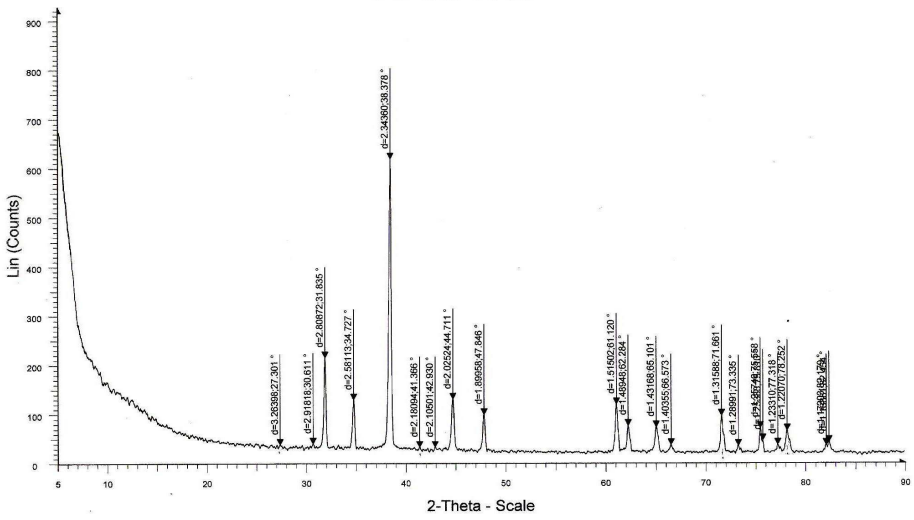

(b)

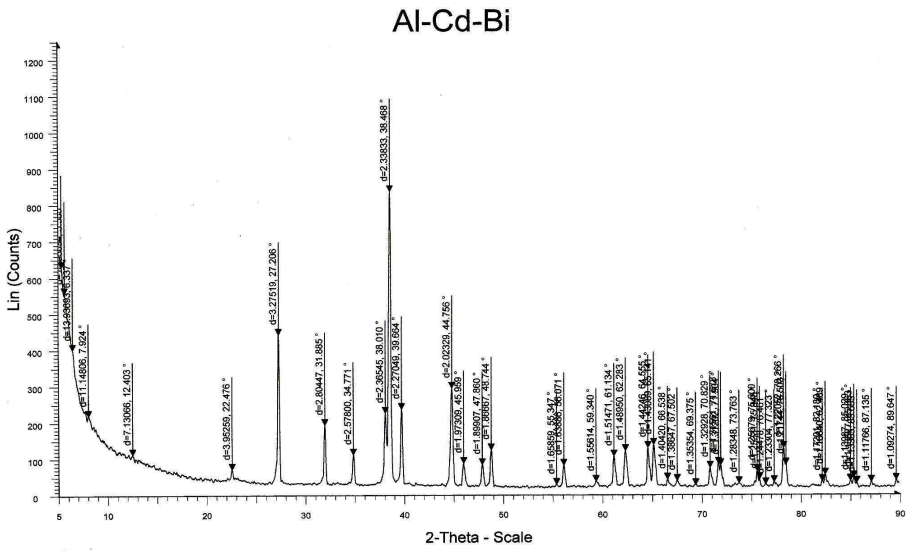

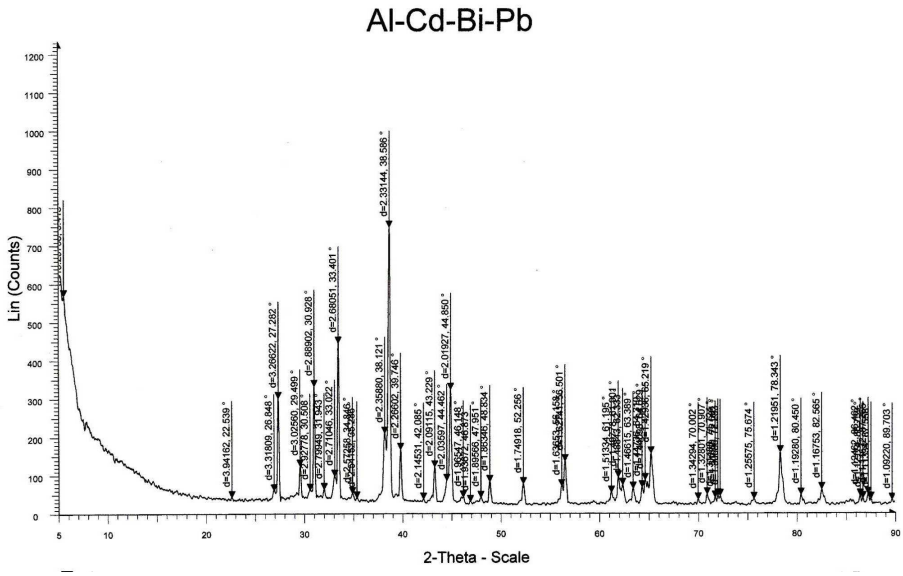

(c)

Fig. 2: XRD patterns of composite alloys (a) Al-Cd; (b) Al-Cd-Bi and (c) Al-Cd-Bi-Pb.

Microscopic view of the composite phases oriented at different growth rates is pictorially illustrated in Figs. 3-6. The lamella habits of the composite phases producing distinct lamellar microstructures from the melt present their relationship with the moderate growth velocity (~2.90 x $10^{-7}m^3s^{-1}$) determined by setting the flow- interval of silicone oil at 5.0 x $10^{-4}m^3$ for 28 min., this particular process of solidification strengthens the composite lamellae to exhibit optimum hardness in the present investigation.

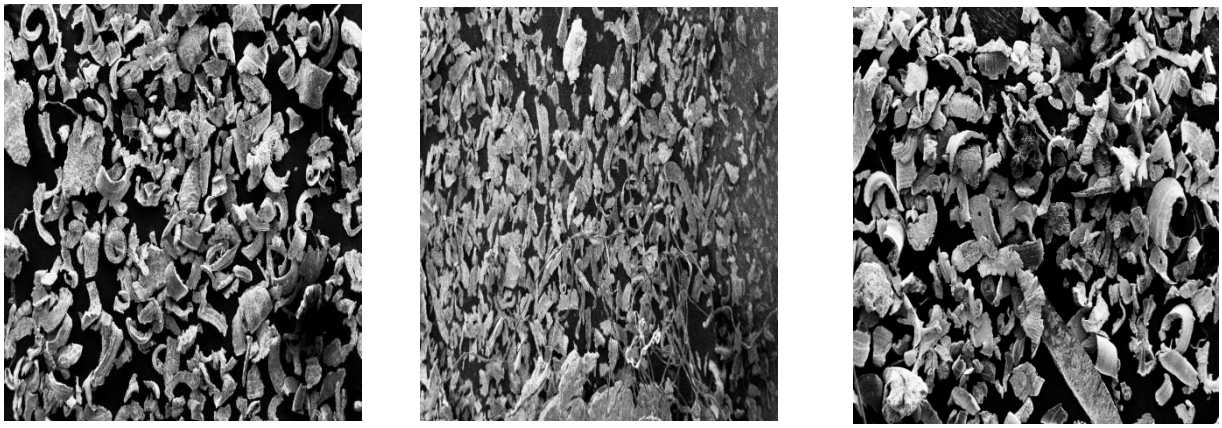

a **b** **c**

Fig. 3: Distorted microstructure of composite phase lamellae in ice bath at ~273 K (1500 x) (a) microstructure of Al-Cd; (b) microstructure of Al-Cd-Bi and (c) microstructure of Al-Cd-Bi-Pb.

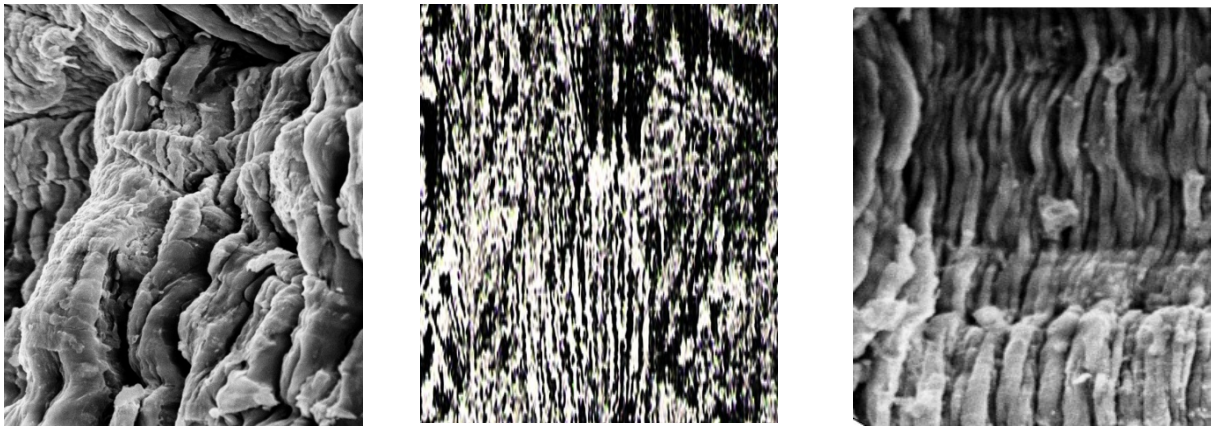

a **b** **c**

Fig. 4: Evolution of composite phase lamellae in growth direction from bottom to top in the fast growth region, 8.10 x $10^{-7}m^3s^{-1}$ (1500 x) (a) microstructure of Al-Cd; (b) microstructure of Al-Cd-Bi and (c) microstructure of Al-Cd-Bi-Pb.

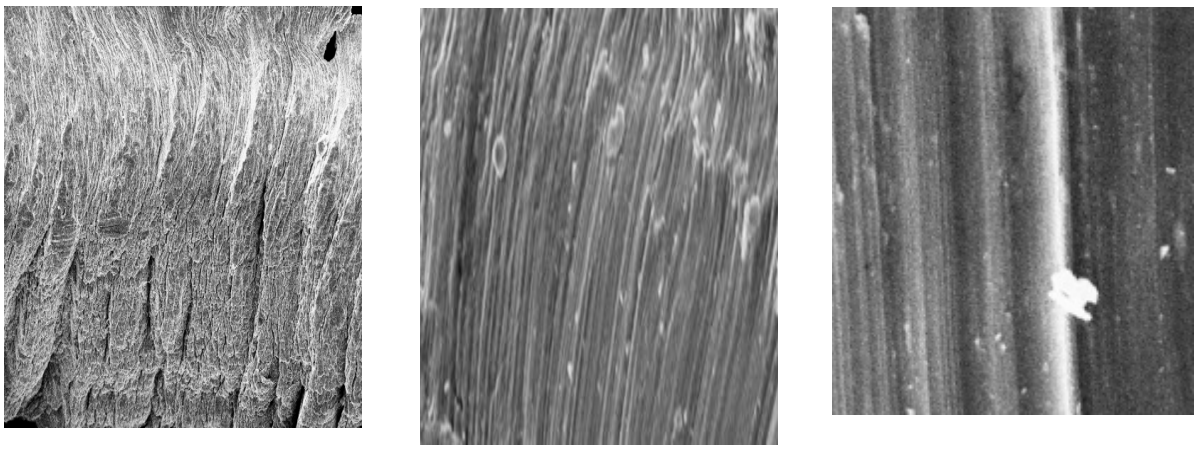

a **b** **c**

Fig. 5: Composite phase lamellae in the growth direction from bottom to top in the slow growth region, 1.71 x $10^{-7}m^3s^{-1}$ (1500 x). (a) microstructure of Al-Cd; (b) microstructure of Al-Cd-Bi and (c) microstructure of Al-Cd-Bi-Pb

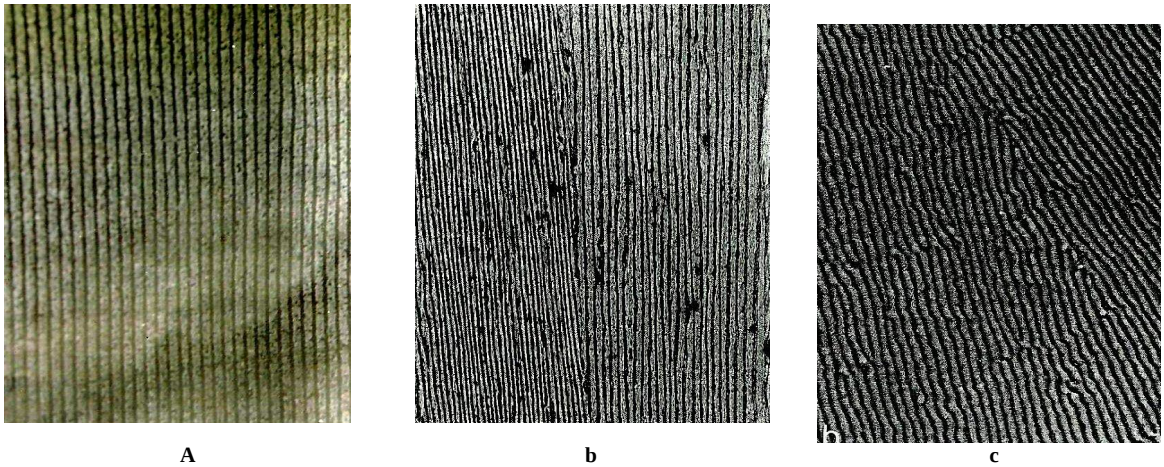

A **b** **c**

Fig. 6: Lamellar composite phase, growth direction from bottom to top in the moderate growth region, 2.90 x $10^{-7}m^3s^{-1}$ (1500 x) (a) microstructure of Al-Cd; (b) Microstructure of Al-Cd-Bi and (c) microstructure of Al-Cd-Bi-Pb

Mechanical parameters computed for tensile, compressive and modulus modes of rupture of composite alloys Al-Cd; Al-Cd-Bi and Al-Cd-Bi-Pb solidified at moderate anisotropic (~2.90 x $10^{-7}m^3s^{-1}$) and isotropic (zero order growth ~ 273 K) growth rates are provided in table 2.

Table 2 : Mechanical parameters* of composite phases at moderate anisotropic (~2.90 x $10^{-7}m^3s^{-1}$) and isotropic (~ 273 K) growth rates

S.No	Specimen	Modulus of rupture Y_{rup}(MPa)	Tensile strength T_{rup}(MPa)	Compressive strength σ_{rup}(MPa)	Elongation percentage
1.	**Al-Cd alloy** anisotropic growth	126.10	140.20	160.30	26
	isotropic growth	70.00	80.60	100.20	13
2	**Al-Cd-Bi alloy** anisotropic growth	96.10	121.40	146.30	20
	isotropic growth	48.40	61.50	86.30	10
3	**Al-Cd-Bi-Pb alloy** anisotropic growth	102.40	118.60	142.30	17
	isotropic growth	38.10	53.40	74.40	08
4	**Al** anistropic growth	60.00	72.90	80.20	17.80
	isotropic growth	51.20	69.10	82.20	13.50
5	**Cd** anistropic growth	4.30	5.40	6.50	5.90
	isotropic growth	3.20	4.60	5.40	4.60
6	**Bi** anistropic growth	5.20	6.90	7.80	3.20
	isotropic growth	2.60	3.80	5.20	1.80
7	**Pb** anistropic growth	7.80	10.28	10.90	14.40
	isotropic growth	6.60	8.50	9.20	11.70

**Averaged values*

The tensile modes of microhardness of the composites at variable velocity (18 intervals) are graphically represented in Fig. 7 (a,b,c) while the compressive and modulus modes of the composites at variable growth velocity are given in table 3.

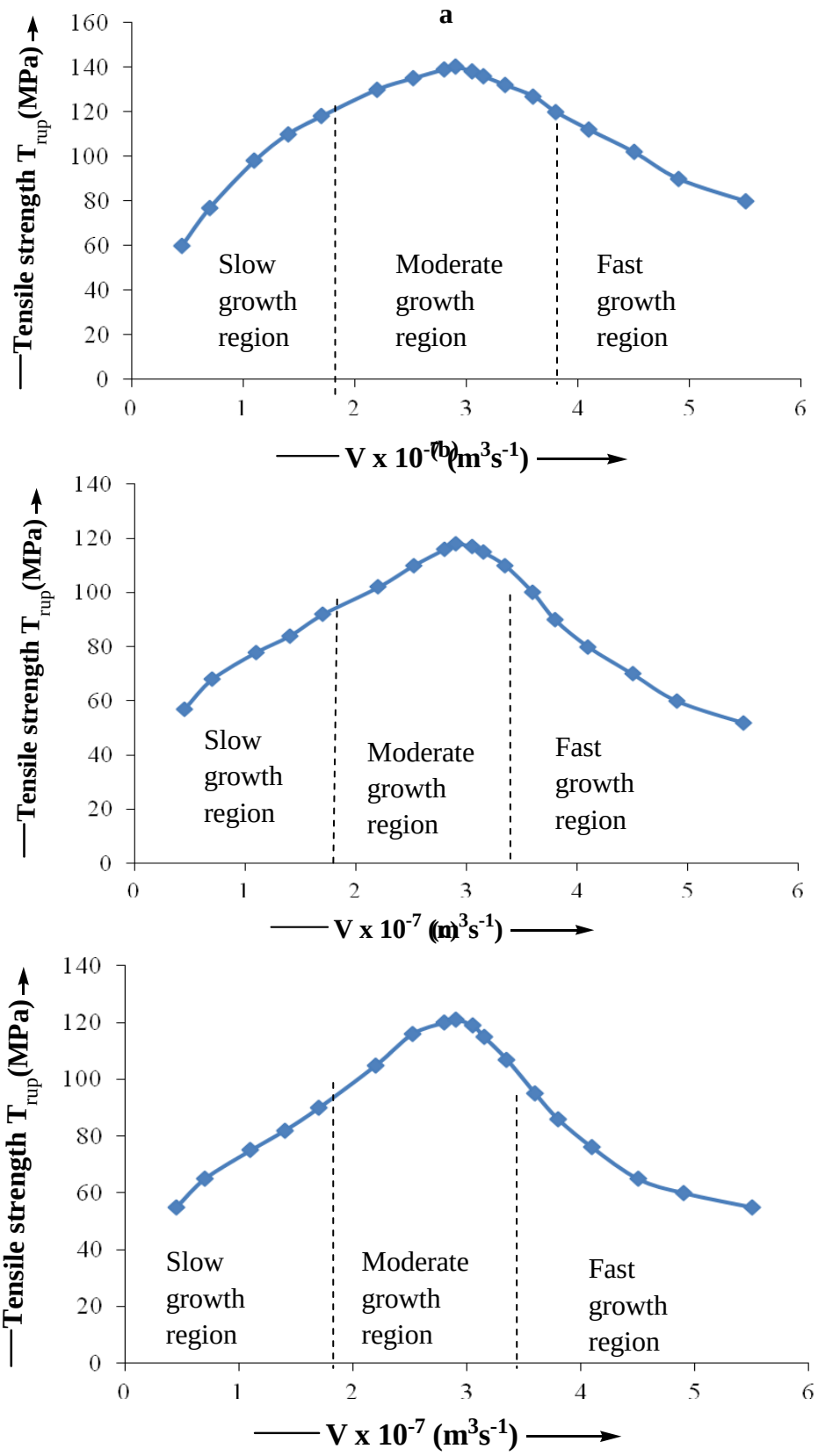

Fig. 7: Variation of Tensile strength with growth velocity for the composite alloys (a) Al-Cd; (b) Al-Cd-Bi and (c) Al-Cd-Bi-P

Table 3: Variation of macrohardness with growth velocity for the composite alloys (a) Al-Cd; (b) Al-Cd-Bi and (c) Al-Cd-Bi-Pb.

(a)

Growth velocity ($V \times 10^{-7} m^3 s^{-1}$)	Compressive strength σ_{rup} (MPa)	Modulus of Rupture Y_{rup} (MPa)
0.45	55.00	57.00
0.70	62.00	68.00
1.10	78.00	78.00
1.40	90.00	84.00
1.70	102.00	92.00
2.20	125.00	107.00
2.52	147.00	120.00
2.80	158.00	125.00
2.90	160.00	126.00
3.05	157.00	124.00
3.15	150.00	120.00
3.35	135.00	109.00
3.60	110.00	98.00
3.80	95.00	90.00
4.10	80.00	78.00
4.50	70.00	68.00
4.90	60.00	59.00
5.50	50.00	53.00

(b)

Growth velocity ($V \times 10^{-7} m^3 s^{-1}$)	Compressive strength σ_{rup} (MPa)	Modulus of Rupture Y_{rup} (MPa)
0.45	64.00	35.00
0.70	71.00	40.00
1.10	85.00	53.00
1.40	94.00	65.00
1.70	100.00	73.00
2.20	116.00	85.00
2.52	128.00	95.00
2.80	140.00	100.00
2.90	142.00	102.00
3.05	140.00	99.00
3.15	135.00	95.00
3.35	124.00	87.00
3.60	112.00	80.00
3.80	100.00	75.00
4.10	92.00	67.00
4.50	86.00	60.00
4.90	70.00	57.00
5.50	65.00	55.00

(c)

Growth velocity ($V \times 10^{-7} m^3 s^{-1}$)	Compressive strength σ_{rup} (MPa)	Modulus of Rupture Y_{rup} (MPa)
0.45	69.00	32.00
0.70	76.00	38.00
1.10	89.00	50.00
1.40	97.00	62.00
1.70	105.00	70.00
2.20	120.00	80.00
2.52	132.00	88.00
2.80	145.00	95.00
2.90	146.00	96.00
3.05	144.00	94.00
3.15	138.00	90.00
3.35	127.00	85.00
3.60	117.00	79.00
3.80	105.00	72.00
4.10	98.00	65.00
4.50	90.00	57.00
4.90	76.00	53.00
5.50	69.00	45.00

The analysis of the experimental observations necessarily involves a physical understanding of the relationship between the growth habits (Figs.3-6) and mechanical parameters (Fig. 7 and Table 2) of the composites Al-Cd; Al-Cd-Bi and Al-Cd-Bi-Pb. A critical examination of Table 2 reveals an important aspect of the investigation that the moderate growth (~2.90 x $10^{-7}m^3s^{-1}$) strengthens the microstructures of the composites approximately two to three fold of their isotropic growth (~273 K) and manifold superior to their constituent phases irrespective of the growth mode whether anisotropic or isotropic. The solidification observation reveals that the variation of the mechanical property over the entire experimental growth velocity range follows the Weibull probability distribution curve (Fig. 7) that furnishes two cut-off points which divide the plot into three regions, namely, (1) slow growth region; (ii) moderate region and (iii) fast growth region. Figure 7 (a-c) indicate that among the growth regions, the moderate growth region appears to be the most probable one for producing the complete lamellar microstructures (modal products) of the composites (Fig 6) wherein microstructural parameters, namely, lamella diameter; lamella length; lamella length distribution; volume fraction of lamellae and the alignment and packing arrangements of lamellae, seem nearly obeying the Gauss distribution. By virtue of the growth process, the composite (Fig 6) manifest mechanical properties (Table 2) which are unique compared to that of their respective isotropic growth in an ice bath (Fig. 3) and their constituent phases (Table 2) which grew out as lamellar cells with aggressive and crossing microstructural parameters producing fragile matrix. The physical significance to be drawn from the plot (Fig. 7) is that the variation of an anisotropic mechanical property over the entire experimental range of growth velocity is an evidence of its dependence as linear, non-linear, and linear respectively in the slow, moderate, and fast growth regions of solidification. The concept implicitly, generates the strength-growth relationship, which follows an identical form of the Weibull distribution curve [5,8,15], since the microstructural parameters follow the distribution, particularly in the slow and fast growth regions (Figs. 3-5). Eventually, the two cut off points occur on the curves corresponding to a lower strength limit in the slow and fast growth regions, and an upper strength limit in the moderate growth region. The latter is equivalent to the theoretical strength of the lamellae, as the microstructural parameters nearly obey Gauss distribution (Fig. 6), in the absence of any internal defects or surface flaws which are responsible for reduced strength.

The ascent in macro mechanical modes of the composites (Fig. 7) in the moderate anisotropic growth region is explained in view of the lamellar growth habits of the composite phases from the melt. The lamellae are fibres practically having no density of dislocations, particularly when developed in the moderate growth region in which they are parallel to each other in an attaching and nonaggressive unidirectional lamina reinforcing the matrix where there is a perfect lamella-matrix bond [16-20]. This leads to an implicit obedience of microstructural parameters to the Gauss distribution. By virtue of the lamellar growth (Fig 6) the composites expresse higher strength ability over the random growth (Figs.3-5) and constituent phases (Table 2), since the lamellae of the modal composite phases are in equilibrium with the matrix resulting in strong lamella-matrix relationship (Fig 6) while Figs.3-5 expresse distorted structures of the composites comprising of aggressive, non-attaching and irregular thin lamellae which produce their fragile lamella [21-24] matrices interdependence.

A comparative study of the macromode strength (Table 2 and Fig. 7) reveals that the compressive mode is slightly higher than the tensile which in turn, slightly exceeds the modulus of rupture ($\sigma_{rup}>T_{rup}>Y_{rup}$) . In view of the strength mode order, an inferential insight may be proposed that the phenomenon of multiphase growth from composite melt influences the lamella's length. In the present case, composite phases would solidify as supercrescent lamellae and the length of each metal-lamella gets shortened during the growth process. Since the complete lamella is an attachment of nonaggressive ductile metal lamellae, the efficiency of the lamellae in stiffening and reinforcing the matrix decreases as the lamella length decreases. Lamella ends play an important role in the fracture of short lamella composites and also in continuous lamella composites, since the long lamellae may break into discrete lengths.

CONCLUSION

The current work generates strength-growth relationship that follows an identical form of Weibull probability distribution curve evolving cut-off points corresponding to a lower strength limit in slow and fast growth regions, and an upper strength limit in moderate growth region. The moderate growth is an experimental evidence for being the most probable one in the domain of solidification modes in structuring the modal microstructure comprising of lamellae reinforcing the matrix where there is a perfect lamella-matrix bond, since the microstructural parameters, namely, lamella diameter; lamella length; lamella length distribution; volume fraction of lamellae and the alignment and packing arrangements of lamellae express their obedience to the Gauss distribution in the moderate growth region. While in the slow and fast growth regions, the mechanical parameters are of similar values because of the microstructural parameters in both the regions follow the Weibull distribution. Moreover, the strength aspect establishes the alloying ability which is more in Al-Cd composite compared to Al-Cd-Bi and Al-Cd-Bi-Pb composites. The thermal analysis reveals thermal stability and liquidus temperatures of the composites. X-ray

diffraction patterns implicity demonstrate that the composites are terminal solidus solutions comprising of physically distinct and mechanical separable materials because no unique X-ray pattern is observed in the composites other than constituent metals.

REFERENCES

[1] D Hull, TW Clyne, An introduction to Composite Materials: IIInd edition (Cambridge University Press, **2008**).
[2] D Hull, TW Clyne, An introduction to Composite Materials: 2nd edition (**1996**).
[3] W D Callister, G David Rethwisch, Composites: Polymer-Matrix composites. Fundamentals of Materials Science and Engineering, 3rd ed. Hoboken, NJ: Wiley (**2008**).
[4] WD Callister Jr., Materials Science and Engineering: An introduction, John Wiley & Sons, Inc (**2004**).
[5] BL Sharma, Parshotam Lal, Growth Reinforcing composite materials from liquidus phase: Mechanical and Microstructural Parameters Relationship Essentially Evincing the Predominance of an Akin Mass composite over the Domain of composition, Metal, Ceramic and Polymeric Composite for various uses, John Cuppolettic (Ed.) ISBN: 1978-953-307-353-8 In Tech (**2011**).
[6] D Hull, An introduction to composite Materials, Cambridge University Press, Cambridge (**1985**).
[7] W Albers, in: H Muller (Ed.), Preparative Methods of Solid State Chemistry, Academic Press, New York (**1972**).
[8] BL Sharma, S Tandon, S Gupta. *Cryst. Res. Technol*. **2009**, **44**, 258-268.
[9] BL Sharma, Parshtom Lal, Monika Sharma, Arun Kumar Sharma. Thermoanalysis of binary condensed eutectic phases envincing molecular interaction. J. Therm Anal. Calorim DOI 10-1007/S/0973-011-1673-8 (**2011**).
[10] DE Ovesienko, GA Alfinster, in: T Arizumi (Ed.), Crystal Growth, properties and Application, springer-verlag, Berlin **1980**, **2**.
[11] R Caram, WR Wilcox, *J. Mater. Process, Manuf. Sci*. **1992**, **1**, 56.
[12] Smock, Doug. "Boeing 787 Dreamliner Represents Composites Revolution." Design News June (**2008**).
[13] CR Tottle, An Encyclopedia of Metallurgy and Materials, LXVI, Macdonald and Evans Ltd., Great Britain (**1984**).
[14] BL Sharma et.al, J. Res. Sch. Lib., *Arch. Appl. Sci. Res.* **2012**, **4**, 111-127, .
[15] "Boeing 787 Dreamliner Long-Range, Mid-size Airliner, USA." Aerospace-Technology.com Net Resources International. 10 Jan. (**2010**).
[16]G R,VD Bhandankkav,BM,Suryvanshi, J. Res. Sch. Lib., Ultrasonic Study of Molecular Interactions in Binary Mixture at 308K(**2012**),1-4
[17]V renganaki, D syamala,R sathyamoorthy, J. Res. Sch. Lib.,Growth,structural, and Spectral Studies on Pure and doped Ammonium (**2012**) 1453-1461
[!8]T thaila and S kumarraman, J. Res. Sch. Lib.,Growth and characterization of Glycine Magnesium Chloride *Single Cyrstal* (**2012**)1494-1501
[19]RJosephine usha,J Arul Martinmani, PSagayaraj, V Joseph, J. Res. Sch. Lib., Synthesis, growth, Optical, Mechanical ,Thermal and surface Studies of ligand base Single Crystal of tri-allythisurea Cadnium Chloride (**2012**)1545-1552
[20] Sofge, Eric. "Boeing's New 787 Dreamliner: How it works." Popular Mechanics, 14 Jan (**2010**).
[21] R Caram, M Banan, WR Wilcox, *J. Cryst. Growth* **1991**, **114**, 249.
[22] R Caram, S Chandrasekhar, WR Wilcox, *J. Cryst. Growth*, **1990**, **106**, 294.
[23] BL Sharma, S Gupta, S Tandon, R Kant, *Mater Chem. Phys*., **2008**, **111**, 423-430.
[24] DR Lide, CRC Handbook of Chemistry and Phsysics, A Ready-Reference book of Chemical and Physical Data 90th ed. CRC Press, London (**2009**).